An automatic algorithm for blink-artifact suppression based on iterative template matching: Application to single channel recording of cortical auditory evoked potentials

Joaquin T Valderrama[1,2,3], Angel de la Torre[4], Bram Van Dun[1,2], Harvey Dillon[1,2,3]

[1] National Acoustic Laboratories, NSW, Australia
[2] HEARing Co-operative Research Centre, Australia
[3] Department of Linguistics, Macquarie University, NSW, Australia
[4] Department of Signal Theory, Telematics and Communications, CITIC-UGR, University of Granada, Granada, Spain

E-mail: joaquin.valderrama@nal.gov.au; joaquin.valderrama@mq.edu.au

Abstract. Artifact reduction in electroencephalogram (EEG) signals is usually necessary to carry out data analysis appropriately. Despite the large amount of denoising techniques available with a multichannel setup, there is a lack of efficient algorithms that remove (not only detect) blink-artifacts from a single channel EEG, which is of interest in many clinical and research applications. This paper describes and evaluates the Iterative Template Matching and Suppression (ITMS), a new method proposed for detecting and suppressing the artifact associated with the blink activity from a single channel EEG. The approach of ITMS consists of (a) an iterative process in which blink-events are detected and the blink-artifact waveform of the analyzed subject is estimated, (b) generation of a signal modeling the blink-artifact, and (c) suppression of this signal from the raw EEG. The performance of ITMS is compared with the Multi-window Summation of Derivatives within a Window (MSDW) technique using both synthesized and real EEG data. Results suggest that ITMS presents an adequate performance in detecting and suppressing blink-artifacts from a single channel EEG. When applied to the analysis of Cortical Auditory Evoked Potentials (CAEPs), ITMS provides a significant quality improvement in the resulting responses. The proposed ITMS algorithm is easy to be implemented, as can be observed in the Matlab script provided as supporting material.

Keywords: artifact removal, single channel EEG, quality enhancement, blinking, brain-computer interface (BCI) games

1. Introduction

The use of electroencephalogram (EEG) signals is nowadays very common in several research fields because of its objective and non-invasive nature [1, 2]. Some of these research fields include neuroscience [3]; evaluation of cognitive factors like attention [4], learning [5] and memory [6, 7]; linguistic development [8, 9]; and diagnosis of cognitive disorders like dyslexia [10], autism [11], and auditory processing disorder [12].

The recorded EEG signals are often contaminated by biological artifacts of different origin, such as eye-blinks, ocular movements (saccades), and muscular and cardiac activity; by non-biological factors like the amplifier noise proportional to the impedance between the electrodes and the scalp; and by electromagnetic fields induced by external sources [13]. In particular, the eye-blink artifact is among the factors that mostly degrades the quality of the EEG signals, especially in the frontal channels [14]. Therefore, the use of signal processing techniques that compensate for this undesired effect is usually necessary.

Blink-artifact removal has been approached from many different perspectives. A comprehensive review of EEG artifact removal techniques can be found in [15]. According to this review, the most used techniques reported in the literature are based on electrooculogram (EOG) subtraction, adaptive filtering, and independent component analysis (ICA). The approach of EOG subtraction methods consists of subtracting from each analyzed EEG channel a proportion of one or more reference EOG channels containing the blink-artifacts (usually vertical and horizontal; and also radial for optimal performance) [16, 17]. The major disadvantages of these methods are that they require additional EOG channels as a reference, and that they do not assume bidirectional contamination, i.e. that the EOGs may also be 'contaminated' by a proportion of the signal of interest, thus part of the signal of interest in the EEG would be cancelled in the subtraction process. These methods are still considered by many authors as the 'gold-standard' because of their simplicity, good performance, and low computational load [18, 19, 20].

Adaptive filtering methods consist of designing the filter parameters that minimize the error between the contaminated and the desired (free of artifact) EEG. In these methods, the filter generates a signal correlated with the artifact, which is then subtracted from the contaminated EEG [21]. These methods also require additional EOG channels as a reference to operate [22].

ICA is based on the linear mixture concept, in which the recorded EEG and EOG channels are modeled as the combination of contributions from different brain and artifact sources [23]. Artifact rejection with ICA involves a complex mathematical process consisting of (a) decomposing the EEG channels into statistically independent components, (b) selecting the components associated with the eye-blink artifact, and (c) recomposing the EEG signals without the selected artifact components [24, 25]. Although ICA can be implemented in a single-channel configuration, the optimal performance of this technique requires the use of several EEG channels [26]. In the

last decade, ICA has become very popular because of its performance [27, 28, 29], and in part, because of its easy implementation as it has been integrated into open-access signal processing toolboxes like EEGLab [30]. However, there is an ongoing debate about the quality of blink-artifact correction when decomposing and recomposing the EEG signals into independent components [18, 31, 32, 33].

In contrast to the large number of techniques available in multichannel applications, there has been little research in developing signal processing techniques to deal with the blink-artifact in single-channel EEG applications. These applications are nowadays very common in the clinic, e.g. estimating hearing thresholds with cortical auditory evoked potentials (CAEPs) [34]; as well as in an increasing number of brain-computer interface (BCI) applications in the fields of research and games, derived from a new generation of low-cost and portable EEG recording devices characterized by using a low number of channels and no access to EOG data [35, 36, 37].

The most relevant techniques to detect blink-events in single-channel EEG applications are based on amplitude-threshold, template matching, and derivatives. Amplitude-threshold based techniques consist of evaluating whether the maximum amplitude within an epoch (i.e., EEG segment containing the signal of interest and noise) exceeds a threshold, which can be set in advance by the user or automatically considering the EEG amplitude distribution [38, 39]. These methods are relatively easy to implement, but they present limitations such as (a) low accuracy, since they cannot distinguish blink-events from other high-amplitude artifacts, e.g. muscular activity or jaw movements [40]; (b) they cannot define the blink-artifact morphology or the EEG interval in which the blink-artifact occurs [41]; and (c) blink-events with the main peak component outside the limits of the epochs cannot be detected [42].

Template matching is a well-known signal processing technique for pattern recognition, which is currently being used in a variety of fields such as image processing [43, 44], signature recognition [45], stock technical analysis [46, 47], automatic classification of seismic activity [48], etc. Methods based on template matching essentially provide a distance representing the similarity between a test signal and a predefined waveform (template). A threshold must be specified for detection purposes. Template matching has been previously used in detecting blink-events in single-channel EEG applications [49, 50]. The major challenges of these methods are (a) the definition of the template, because the performance of the method would be affected if the blink-artifact morphology of a test subject does not match the template; and (b) the definition of the threshold. Both papers solve these issues by asking the user to set the threshold manually and by using a library consisting of a number of templates of different morphology. These solutions present the inconveniences of requiring expertise from the user, which makes the method inconsistent worldwide; and dependent on the library of templates selection.

A third approach for blink-artifact detection is based on the use of derivatives. These methods assume that the blink-artifacts present a triangular-shape morphology, and aim to detect abrupt changes by analyzing the derivative function of the raw

EEG [51]. The multi-window summation of derivatives within a window (MSDW) technique requires the user to set a threshold manually, but it does not require a database of templates and is able to estimate the EEG intervals in which the blink-artifacts occur. MSDW presents better accuracy in detecting epochs containing blink-events compared to the amplitude-threshold and the traditional template matching approaches.

The major limitation of the aforementioned methods is that they allow detection, but not correction, of blink-artifacts. These methods have been typically used to detect and reject epochs contaminated with blink-artifacts, which eventually leads to the undesired loss of useful data [42, 16]. Unfortunately, methods able to detect and correct blink-artifacts from a single channel EEG are scarce.

The objective of this paper is to describe and evaluate a novel approach for detection and suppression of blink-artifacts in a single-channel EEG signal. The procedure is based on Iterative Template Matching and Suppression (ITMS). First, detection of blink-events is carried out by an iterative implementation of template matching, using a predefined blink-artifact template in the first iteration, and a blink-artifact waveform estimated from the test subject in the following iterations. Second, a blink-artifact signal is modeled considering the blink-artifact waveform of the subject and the positions and amplitudes of the detected blink-events. Finally, the signal modeling the blink-artifact is subtracted from the raw EEG to obtain the denoised EEG.

The performance of the ITMS method is compared with the MSDW technique in terms of both blink-artifact detection and suppression. A software script programmed in Matlab (The Mathworks, Inc., Natick, MA) that implements the ITMS algorithm is available as supplementary material (appendix A).

2. Iterative Template Matching and Suppression (ITMS)

This section describes the mathematical formulation for the Iterative Template Matching and Suppression (ITMS) algorithm, which includes the blink-artifact estimation and its suppression from the recorded EEG. The ITMS method assumes that the recorded EEG $y(n)$ is the summation of three uncorrelated processes: the blink-artifact $x_{blink}(n)$, the signal of interest $x_{signal}(n)$, and the noise $x_{noise}(n)$ associated with the recording procedure,

$$y(n) = x_{blink}(n) + x_{signal}(n) + x_{noise}(n), \tag{1}$$

where $n = 0, \ldots, N-1$, and N is the total number of samples in the EEG. The objective of ITMS is to obtain an estimate of the blink-artifact process $\widehat{x}_{blink}(n)$ in order to provide an enhanced EEG in which the blink-artifact is suppressed.

The blink process is assumed to be linear and time-invariant (LTI), i.e. each blink-event produces an additive artifact with the same template (even though with unknown amplitude), and the blink-artifact is the sum of the artifact associated with each individual event. The blink-artifact can therefore be modeled as the convolution of a blink-artifact template $h(n)$ ($n = 0, \ldots, L-1$) with K impulses (at positions m_k

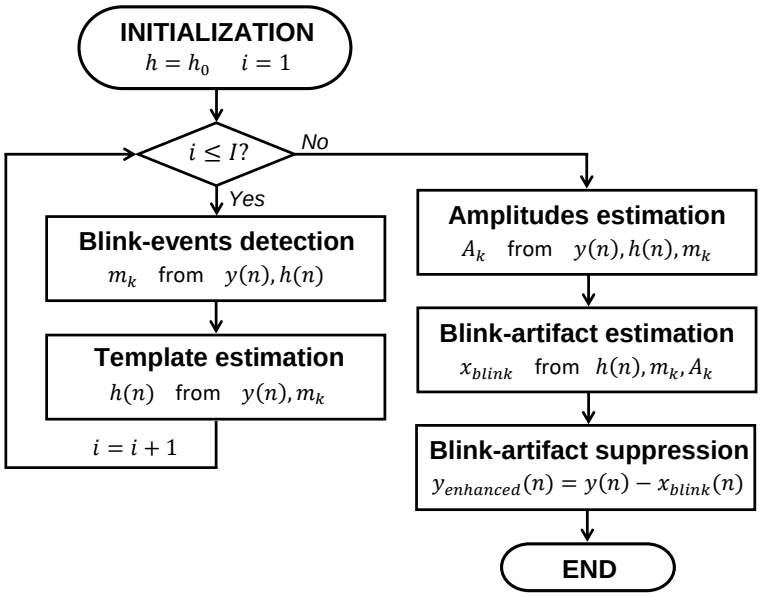

Figure 1. Iterative Template Matching and Suppression algorithm flowchart.

and with amplitudes A_k) representing the blink-events

$$\widehat{x}_{blink}(n) = h(n) * \sum_{k=1}^{K} A_k \delta(n - m_k) = \sum_{k=1}^{K} A_k \cdot h(n - m_k), \tag{2}$$

where L is the number of samples of the blink-artifact template, K is the number of blink-events, $*$ represents the convolution operator and $\delta(n)$ is the unitary impulse at $n = 0$. As a final assumption, the amplitude of the blink-artifact is accepted to be relatively large compared with the other signals, which is consistent with the artifacts usually observed in EEG recordings.

ITMS estimates the blink-artifact (i.e. the template $h(n)$, and the parameters A_k, m_k describing the blink-events) through an iterative process, in which $h(n)$ is initialized with a predefined template $h_0(n)$. The estimation of the blink-artifact is iteratively performed by (a) detecting the blink-events (through cross-correlation of the recorded EEG with the template representing the blink-artifact) and (b) re-estimation of the blink-artifact template (through averaging the EEG portions corresponding to the blink-events). After the convergence of the iterative process, the template $h(n)$ and the blink-event parameters (m_k and A_k) provide the blink-artifact estimate $\widehat{x}_{blink}(n)$, which can be subtracted from the EEG.

Figure 1 shows a flowchart of the ITMS algorithm. At the first iteration, $h(n)$ is initialized with $h_0(n)$. At each iteration, the blink-events are detected by analyzing the local maxima of the cross-correlation function of the recorded EEG $y(n)$ and the current template $h(n)$. The detected blink-events at positions m_k are used to average the portions of EEG associated to each blink-event in order to re-estimate the blink template $h(n)$. This way, at each new iteration a better detection of the blink-events

provides a better estimation of the blink-template. After I iterations, the template $h(n)$ and the positions of the blink-events m_k are used for estimating the amplitudes of the blink-events A_k. Finally, the template and the blink-event parameters ($h(n)$, m_k and A_k) are used for estimating the blink-artifact $\widehat{x}_{blink}(n)$ and for suppressing it from the EEG.

This procedure provides an estimation of the blink-template specifically adapted to the subject and to the recording conditions (i.e. electrode impedances, specific location of the recording electrodes, etc.). As a consequence, the blink-artifact will be optimally suppressed from the EEG. The processes involved in the proposed method are described in detail below.

2.1. Blink-events detection

At each iteration i, detection of blink-events m_k is carried out through the cross-correlation between the EEG $y(n)$ and the current blink-template $h(n)$. The cross-correlation can be implemented by filtering $y(n)$ with the matched-filter (consisting in the time-reversed version of $h(n)$) [52]. Since every blink-event produces a local maximum in the matched-filter output, the local maxima of this function are candidates to be categorized as blink-events. The matched-filter output can be obtained as,

$$z(n) = y(n) * h(L-1-n) \tag{3}$$

and it provides the cross-correlation between $y(n)$ and $h(n)$ with a delay when a causal implementation of the matched-filter is applied (i.e. there is a delay of $L-1$ samples between each impulse generating an artifact and the corresponding local maximum in $z(n)$, since $h(L-1-n)$ is used instead of $h(-n)$).

Let Z_{0j} and m_{0j} be, respectively, the amplitudes and positions of the local maxima in $z(n)$,

$$Z_{0j} = z(m_{0j}) \quad \forall\ m_{0j} \text{ verifying that } \quad z(m_{0j}) > z(m_{0j} \pm 1) \tag{4}$$

where $j = 1, \ldots, J$, and J is the total number of local maxima in $z(n)$. On one hand, the blink-events generate local maxima with large (and positive) amplitudes in the cross-correlation function, according to the amplitude distribution of the blink-events. On the other hand, noise and other uncorrelated signals (with waveforms different to that of the template) produce a large number of random local maxima with smaller amplitudes. Therefore, the histogram of the local maxima $\{Z_{0j}\}$ is expected to show a large and narrow Gaussian mode centered at zero (corresponding to the local maxima associated to noise and other uncorrelated signals) and a wider mode with larger amplitudes (corresponding to the blink-events).

Categorization of local maxima candidates as blink-events or uncorrelated signals is carried out through the analysis of the histogram of local maxima. Following the approach proposed by Kim and McNames (2007) for automatic spike detection in extracellular neural recordings [53], the histogram is smoothed with a Gaussian kernel (with a 15% of the interquartile interval as bandwidth); the maximum of the smoothed

histogram is associated to the mode corresponding to the uncorrelated signals, and the following minimum of the smoothed histogram (on the side of positive amplitudes) is used as threshold, T. The detected blink-events correspond to those local maxima Z_k with amplitude greater than the threshold,

$$Z_k = z(m_{0k}) \quad \forall\ m_{0k} \text{ verifying that } \begin{cases} z(m_{0k}) > z(m_{0k} \pm 1) \\ z(m_{0k}) > T \end{cases} \tag{5}$$

and the beginning of each detected blink-event is obtained as:

$$m_k = m_{0k} - L + 1 \tag{6}$$

by compensating the delay of $L-1$ samples from the corresponding local maxima at m_{0k}, where $k = 1, \ldots, K$, and K is the number of detected blink-events. At the end of this section, the procedure for detecting the blink-events is illustrated with an example.

2.2. Estimation of the blink-artifact template

The template $h(l)$ (with $l = 0, \ldots, L-1$) is estimated from the EEG $y(n)$ and the positions of the detected blink-events m_k. In order to estimate the template, the segments of the EEG corresponding to the detected blink-events are organized in a $K \times L$ matrix,

$$\mathbf{Y} = [y_{k,l}] \qquad y_{k,l} = y(m_k + l). \tag{7}$$

In an hypothetical situation with accurate detection (each m_k corresponds to a blink-event) the estimation would be carried out by a simple average of the EEG segments (i.e. by synchronized averaging),

$$h(l) = \frac{1}{K} \sum_{k=1}^{K} y_{k,l}. \tag{8}$$

However, detection errors (for example: some low amplitude peaks corresponds to noise; high amplitude impulsive noise produces high amplitude local maxima in the cross correlation) would result in inaccurate estimates of $h(l)$ (and therefore in an inaccurate detection of the blink-events in the iterative procedure). In order to prevent this problem, the template is estimated as a weighted average:

$$h_w(l) = \sum_{k=1}^{K} w_k \cdot y_{k,l} \tag{9}$$

where w_k are weights included to modulate the contribution of each sample to the average. In this work, the weights originate from a Hamming window:

$$w_k = \begin{cases} 0 & \text{if } \ r_l(k) < 0.25K \ \text{ or } \ r_l(k) > 0.75K \\ 0.54 - 0.46 \cos\left(4\pi \frac{r_l(k) - 0.25K}{K-1}\right) & \text{otherwise} \end{cases} \tag{10}$$

where $r_l(k)$ is the rank of $y_{k,l}$ in the set $\{y_{1,l}, y_{2,l}, \ldots, y_{K,l}\}$ (i.e. the position of $y_{k,l}$ after sorting them‡). This way, the estimation of the impulsive response $h(l)$ is a weighted

‡ Because of the symmetry of the Hamming window, the weights w_k are the same when sorting in ascending or descending order.

average where all those values outside the percentiles 25-75 do not contribute, and those between these percentiles do contribute with a weight modulated by a Hamming window (the contribution of the median is maximum), and therefore the estimation of the impulsive response shares the advantages of a median-based estimation (small influence from outliers [54]) and those of a mean-based estimation (a group of samples contributes to the estimation). The mean of the resulting signal is subtracted, 20 Hz low-pass filtered (4^{th} order, Butterworth) and a linear fade-in/out of 200 ms is applied in order to remove DC level, smooth the signal and avoid discontinuities at the beginning and at the end of the template. Finally, the estimated impulsive response is normalized,

$$h(l) = \frac{h'_w(l)}{\sqrt{\sum_{l=0}^{L-1} h'^2_w(l)}}, \tag{11}$$

where $h'_w(l)$ is the demeaned, low-pass filtered and faded-in/out version of $h_w(l)$.

The initial template $h_0(n)$ used in this study was obtained by averaging and normalizing the blink-artifact waveforms identified in a cohort of 14 normal hearing adults (8 males, 43.26 ± 7.18 yr). The detailed procedure that we followed to obtain $h_0(n)$ is provided as supplementary material (appendix B). According to the morphology of the blink-artifact, the duration of the template was set to 1400 ms.

2.3. Blink-artifact amplitudes

The amplitudes A_k of each blink-event are estimated from the EEG $y(n)$, the blink-artifact template $h(n)$ and the positions m_k of the identified blink-events. Taking into account the model of the EEG in equation (1), and since the matched-filter enhances the blink-events and attenuates the contribution of the other signals, the matched-filter output can be approximated as:

$$z(n) \approx x_{blink}(n) * h(L-1-n) = \sum_{k=1}^{K} A_k h(n-m_k) * h(L-1-n) \tag{12}$$

From the definition and properties of the autocorrelation function $R_h(n)$ of the impulsive response,

$$R_h(n) = h(n) * h(-n) \qquad h(n-m) * h(-n) = R_h(n-m) \tag{13}$$

the matched-filter output can be approximated as:

$$z(n) \approx \sum_{k=1}^{K} A_k R_h(n-m_k-L+1) \tag{14}$$

Finally, if the matched-filter output is evaluated at the local maxima associated with the blink events, we obtain K equations (one for each detected blink-event):

$$Z_k = z(m_{0k}) = z(m_k+L-1) \approx \sum_{k'=1}^{K} A_{k'} R_h(m_k - m_{k'}) \tag{15}$$

If the blink-events do not overlap (i.e. the minimum distance between successive m_k positions is greater than L), the term $R_h(m_k - m_{k'})$ is null when $k \neq k'$, and

equal to 1 when $k = k'$ (because $h(n)$ is normalized). In that case, the amplitudes could be directly estimated as the value of the matched-filter output evaluated at the corresponding maximum ($A_k = Z_k$). However, when the blink-events are overlapped, the local maxima of the matched-filter output are affected by the overlapping events and the K equations in (15) should be worked out in order to estimate the amplitudes. These K equations can be written in matrix form:

$$\mathbf{Z} \approx \mathbf{R_h} \cdot \mathbf{A} \tag{16}$$

where $\mathbf{Z}$ is a K-elements vector including the local maxima of the matched-filter output for each detected blink-event, $\mathbf{A}$ is a K-elements vector with the amplitudes of the blink-events to be estimated, and $\mathbf{R_h}$ is a $K \times K$ matrix including the autocorrelation function evaluated at $(m_k - m_{k'})$ for each k, k' between 1 and K:

$$\mathbf{R_h}(k, k') = R_h(m_k - m_{k'}) \tag{17}$$

Note that $\mathbf{R_h}$ is a quasi-diagonal symmetrical matrix, with ones in the main diagonal, values between -1 and 1 outside the diagonal, and null values for non-overlapping events (i.e. when $|m_k - m_{k'}| > L$). Since overlapping of blink-events is expected to affect only a few adjacent events, only a few diagonals (in addition to the main diagonal) are expected to be non-null. Therefore, despite the size of the $\mathbf{R_h}$ matrix, inverting it does not require a large computational load and the estimation of the amplitudes can easily be obtained as:

$$\mathbf{A} = (\mathbf{R_h})^{-1} \cdot \mathbf{Z} \tag{18}$$

2.4. Blink-artifact suppression

When both the blink template (described by $h(n)$) and the blink-events (described by A_k and m_k) are estimated, the signal describing the blink-artifact can be estimated as:

$$\widehat{x}_{blink}(n) = \sum_{k=1}^{K} A_k h(n - m_k) \tag{19}$$

and the enhanced EEG can be estimated by suppressing the blink-artifact estimate:

$$y_{enhanced}(n) = y(n) - \widehat{x}_{blink}(n). \tag{20}$$

The performance of the ITMS method is illustrated with an example included in Figure 2. The EEG was recorded from a normal hearing adult (female, 30 yr). Figure 2.A shows a segment of an EEG, $y(n)$, in which three blink-events can be identified (blue line). The orange line represents the matched-filter output, $z(n)$. The delay between the blink-events and the corresponding maxima in the matched-filter output can be observed. The local maxima of $z(n)$ (indicated with black diamonds) are blink-event candidates.

Figure 2.B shows the normalized histogram of the amplitudes of the local maxima (Z_{0j}), and the kernel-based smoothed histogram. This histogram shows a bimodal distribution with a large mode around zero, representing the signals not correlated

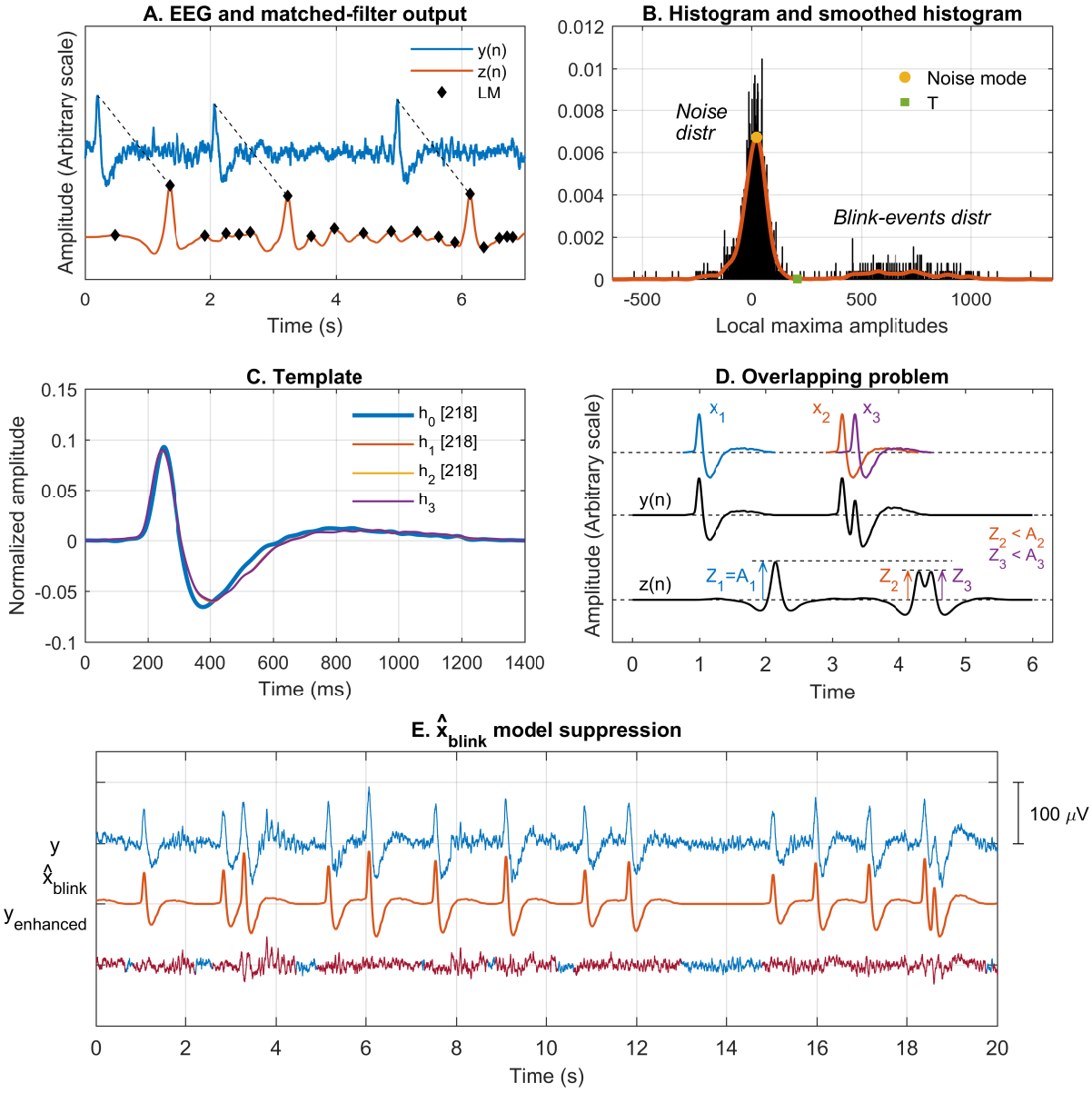

Figure 2. Details of the ITMS process. [A] Raw EEG (blue) and output of the matched-filter function $z(n)$ (orange). Local maxima of $z(n)$ (black diamonds) are blink-event candidates. [B] Histogram of the local maxima amplitudes (Z_{0j}), and kernel based smoothed histogram. The threshold (T) that separates the noise and the blink-events distributions is represented with a green square. [C] Initial template ($h_0(n)$) and blink-artifact waveforms obtained in each iteration ($h_1(n)$ to $h_3(n)$). The total number of blink-events detected in each iteration is shown in brackets. [D] Simulation of amplitudes estimation in overlapping blink-events. [E] Suppression of the estimated blink-artifact model ($\widehat{x}_{blink}$) from the raw EEG leads to an enhanced EEG.

with the blink template (noise and other signals); and a wider mode with larger amplitudes, representing the blink-events. The ITMS algorithm sets the threshold T that separates these two modes as the first local minimum of the smoothed histogram after the maximum corresponding to the noise mode. The local maxima candidates are categorized as blink-events if their amplitude is greater than the threshold.

Figure 2.C shows the waveform morphology of the initial template $h_0(n)$ used in this study (thick blue line) and the blink-artifact templates estimated in the first three iterations ($h_1(n)$ to $h_3(n)$). This figure shows the fast convergence of the ITMS method.

Figure 2.D illustrates that the amplitudes A_k can be estimated as the value of the corresponding local maximum Z_k when the blinking-events are not overlapped, but not when they are overlapped. The top row shows three equal blink-artifact waveforms used to generate a synthesized EEG, the second signal shows the synthesized EEG $y(n)$ and the third signal is the matched-filter output $z(n)$. The first blink x_1 is not overlapped, and therefore $Z_1 = A_1$. However, due to the overlapping of the other two blinks, the amplitudes of the matched-filter output (Z_2 and Z_3) are different than those of the blinks (A_2 and A_3). In general, some degree of overlapping among blinks is expected and an accurate determination of the amplitudes requires an estimation using the proposed method.

Figure 2.E shows an example of a segment of an EEG $y(n)$ where a number of blink-events can be identified (top), the estimated blink-artifact $\widehat{x}_{blink}(n)$ (middle), and the enhanced EEG in which the blink-artifact has been suppressed (bottom). The modified segments in the EEG are shown in red color in the $y_{enhanced}(n)$ signal. This figure shows that the portions of the EEG with no detected blink-events remain unaltered.

The experimental material presented in the assessment section, along with the example shown in figure 2, provide the verification of the initial assumptions: for a given EEG recording, the blink-artifact can be modeled as a LTI process, i.e. the blink-artifact template is stable; the amplitude of the blinking-events fluctuates in a relatively wide range; and the amplitude of the blinking-artifact is relatively large compared with the other signals in the EEG.

3. Assessment

The performance of the ITMS method was evaluated and compared from a double perspective: first, we assessed the ability of ITMS to detect blink-events using synthesized data; and second, we evaluated using real data the effect of suppressing blink-artifacts with ITMS to improve the quality of the CAEP. This section presents the methods and results of these two experiments.

3.1. Subjects

Forty-four normal hearing adults participated in this study (21 males, 44.38 ± 6.95 yr). All participants showed normal hearing sensitivity at test frequencies 0.25, 0.5, 1,

2, 3, 4, 6, and 8 kHz. Hearing thresholds were estimated in 2 dB steps with an Interacoustic AC40 audiometer (Interacoustics A/S, Middelfart, Denmark). All subjects were informed about the test protocol, gave written consent to participate, and were paid at the end of the session to cover trip expenses. From the full set of 44 subjects tested, 14 subjects (7 males, 43.64 ± 7.30 yr) were randomly selected for estimating the predefined blink-artifact template $h_0(n)$ (details in appendix B), and the remaining 30 subjects (14 males, 44.73 ± 6.88 yr) were used in the assessment experiments.

3.2. EEG recording and analysis

The EEG recording protocol consisted of the presentation of auditory stimuli to the subjects and the recording of their associated neural response through surface gold-plated electrodes placed on the high-forehead (active), middle-forehead (ground), and right mastoid (reference). The EEG was recorded using the SmartEP auditory evoked potentials recording system and the Continuous Acquisition Module (SmartEP-CAM, Intelligent Hearing Systems, Miami, FL). The sampling frequency was 1 kHz, the gain of the preamplifier was set at 10,000, and the cut-off frequencies for the bandpass analogue filters were [1-300] Hz. The auditory stimulus consisted of a 170 ms duration /da/ synthesized in Praat [55] with a sampling frequency of 44,100 Hz. The /da/ stimulus was exported to Matlab in order to generate the stimulation sequence, which consisted of 250 repetitions of the /da/ stimulus, presented at 75 dB sound pressure level (SPL), at a fixed rate of 0.66 Hz. Thus, the duration of the sequence was about 380 seconds. The stimulation sequence was delivered monaurally on the right ear through the ER-3A insert earphones (Etymotic Research, Inc., Elk Grove Village, IL), which were connected to a Fireface UCX audio soundcard (RME Audio, Haimhausen, Germany). Stimulus level was calibrated by a type HA2 artificial ear 2-cc acoustic coupler connected to a type 4144 pressure microphone, which was connected to a type 2636 measuring amplifier through a type 2639 preamplifier cable (Brüel & Kjær Sound & Vibration Measurement A/S, Nærum, Denmark). During the EEG recording session, the subjects were lying on a comfortable couch, with their neck and shoulder muscles relaxed, while watching a movie of their choice in silent mode with subtitles. The subjects were asked to keep still during the test and to blink normally. The recording sessions took place in an electromagnetically-shielded booth at the National Acoustic Laboratories (Sydney, Australia). Analysis of recorded signals was carried out by custom scripts developed in Matlab (R2015b), using the Signal Processing and the Statistics and Machine Learning Toolboxes.

This protocol is in accordance with the National Statements on Ethical Conduct in Human Research and was approved by the Macquarie University (Ref 5201400862) and by the Australian Hearing (Ref AHHREC2014-5) Human Research Ethics Committees.

3.3. Experiment 1. Detection of blink-events

3.3.1. Methods Evaluating detection of blink-events from a single frontal EEG channel is a problem because the position of the blink-events in the EEG is not known. This handicap can be solved using synthesized data. In this experiment, we artificially synthesized a number of EEGs with similar noise characteristics as real EEGs, but with the advantage that the position of the blink-events was known in advance.

The artificial EEGs were synthesized from real EEG data collected in 10 subjects (5 males, 43.70±7.23 yr). These subjects were selected from the subset of 30 subjects for presenting large-amplitude blink-artifacts. In each subject, one EEG was synthesized consisting of noise and 300 blink-events. Each EEG was generated in three SNR conditions by modifying the level of noise with respect to the level of the blink-artifacts (signal). The evaluated SNRs were +10 dB, +5 dB, and 0 dB. The noise distributions of the synthesized EEGs consisted of real EEGs after removing all segments containing suspected blink-events after visual inspection. Visual inspection was repeated at least twice, and the selected EEG segments were joined with a 100 ms cosine-square overlapping. This procedure was followed to ensure that the noise distribution of the synthesized EEGs were similar to those of real EEGs, e.g. similar spectral density, non-stationary time-series, etc. The 300 blink-events of each synthesized EEG corresponded to 30 different blink-artifact waveforms of 1.4 s duration (0.25 s pre- and 1.15 s post-local maximum) extracted from the real EEG, each of them used 10 times. The 300 blink-events were randomized, amplitude-normalized, and distributed to synthesize the artificial EEG. The distribution of the inter-blink-interval (time in milliseconds between the onsets of adjacent blink-events) was a $\sim N(2000, 600)$ distribution, i.e inter-blink-intervals followed a Normal distribution with a mean of 2000 milliseconds and a standard-deviation of 600 milliseconds. The distribution of the blink-event amplitudes A_k followed a $\sim N(55, 14)$ distribution. These parameters approximate the real blink-event distributions observed in the 10 analyzed subjects.

The performance of ITMS in detecting blink-events in synthesized EEGs was compared with MSDW [51], a technique that was specifically conceived to detect blink-events from a prefrontal EEG channel. ITMS was implemented as described in section 2 of this paper, using 3 iterations ($I = 3$). MSDW was implemented using the Matlab toolbox provided by the authors [51]. Unlike ITMS, which includes an automatic procedure to estimate the optimal threshold that separates the noise and the blink-events distributions (T), MSDW requires the user to select this threshold manually. We evaluated the performance of MSDW at the threshold suggested by the authors (threshold equal to 130) and at the threshold that we found most appropriate in the tests we did with real EEGs (threshold equal to 80).

The same synthesized EEGs were used in the two techniques for detection purposes. Detection consisted of classifying the blink-events as: true-positive (TP), when the method correctly detected the blink-event; false-negative (FN), when the method did not detect a blink-event; and false-positive (FP), if the method returned a detected

	ITMS			$MSDW_{80}$			$MSDW_{130}$		
SNR	+10 dB	+5 dB	0 dB	+10 dB	+5 dB	0 dB	+10 dB	+5 dB	0 dB
TPR	99.47	97.50	85.00	93.27	91.47	88.90	55.07	57.40	60.87
FPPS	3.3e-4	0.0027	0.0113	9.9e-4	0.0181	0.259	1.7e-4	8.3e-4	0.0219

Table 1. True positive rate (TPR) in percentage (%) and false positives per second (FPPS) obtained at different SNRs with the ITMS method evaluated at the automatic threshold T, and with the MSDW method evaluated at the thresholds equal to 80 ($MSDW_{80}$) and equal to 130 ($MSDW_{130}$).

blink-event when that blink-event was not actually present. The TP, FN, and FP parameters were calculated for each method in the three SNRs at different thresholds in order to generate a receiver operating characteristic (ROC) curve for each analysed SNR. In ITMS, the thresholds varied percentage-wise in terms of the automatic threshold estimate (T): from $0.02 * T$ to T, in steps of $0.02 * T$; and from T to maximum value of Z_{0j}, in steps of $0.02 * (\max\{Z_{0j}\} - T)$. In MSDW, the thresholds varied from 2 to 200, in steps of 2. The ROC curves typically show the true positive rate ($TPR = \frac{TP}{TP+FN}$) against the false positive rate ($FPR = \frac{FP}{FP+TN}$). However, since the ITMS and MSDW methods are not being evaluated for their accuracy in not detecting a blink-event when a blink-event is not present, the true-negative (TN) concept does not make sense in the context of this experiment. Therefore, the ROC curves in this experiment are expressed in terms of TPR against false positives per second ($FPPS$), calculated as the ratio between the number of false positives and the total duration in seconds of the synthesized EEGs.

3.3.2. Results Figure 3.A shows an example of a 30 seconds EEG artificially synthesized at +10 dB SNR (top), +5 dB SNR (middle), and 0 dB SNR (bottom). Figures 3.B-D show the ROC curves for the ITMS (dark gray) and the MSDW (light gray) methods in the three analysed SNRs. These plots show that (a) both methods improve their performance as the SNR of the synthesized EEGs increases; and (b) the ITMS method presents a TPR higher than MSDW for any given FPPS in the three SNR conditions.

Table 1 shows the performance of ITMS evaluated at the automatic threshold T, and MSDW evaluated at a thresholds equal to 80 ($MSDW_{80}$) and 130 ($MSDW_{130}$), in terms of TPR and FPPS obtained at different SNRs. These results are also highlighted in figure 3 as dark-gray stars (ITMS) and light-gray stars ($MSDW_{80}$). The TPR and FPPS results for $MSDW_{130}$ are outside the limits of interest of the figure. The results shown in this table and the ROC trends in figure 3 point out that: (a) the performance of $MSDW_{130}$ is inefficient, i.e. the TPR is particularly low in the three SNR scenarios; (b) setting the threshold manually in $MSDW_{80}$ does not always result into optimal performance, as it seems to be adequate in the +5 dB SNR scenario, but it is inefficient

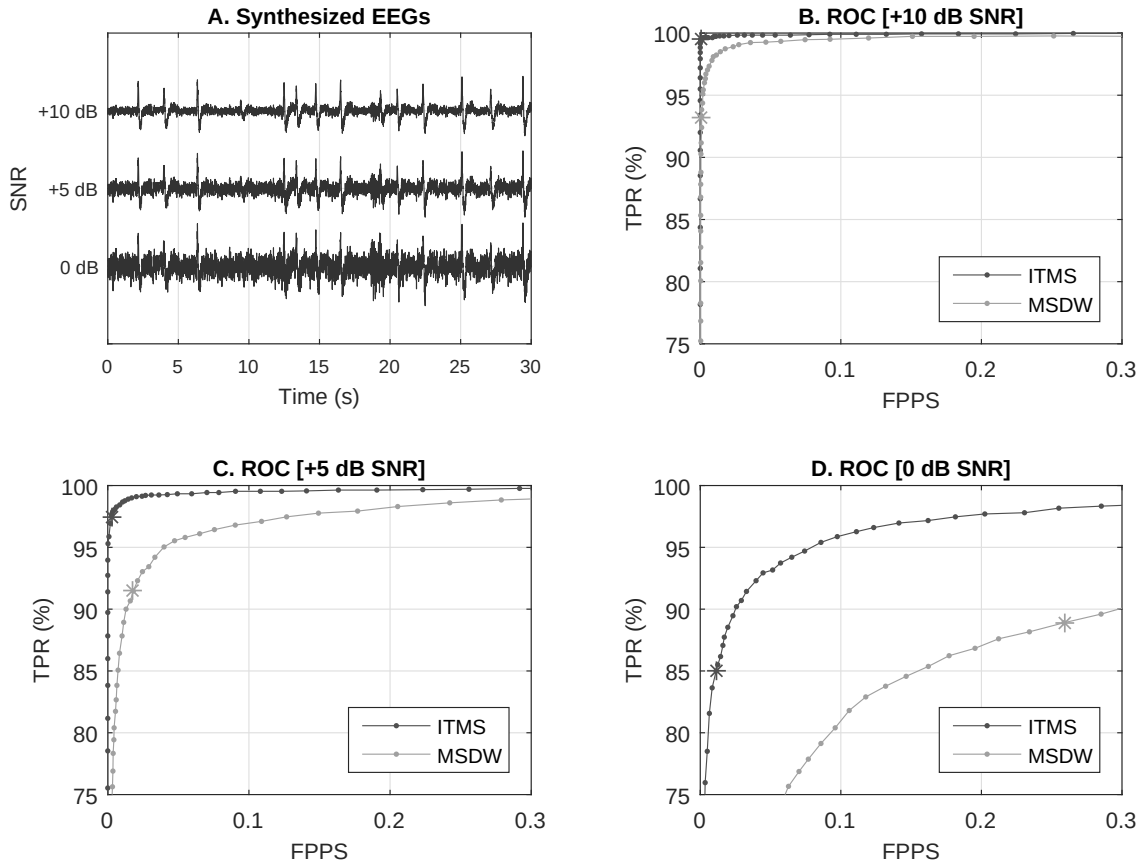

Figure 3. (A) Example of a 30 seconds EEG synthesized at different SNRs. (B-D) ROC curves for the ITMS (dark gray) and MSDW (light gray) methods at +10 dB SNR, +5 dB SNR, and 0 dB SNR. The stars in the chart show the performance of the ITMS method at the automatic threshold (T), and the MSDW method at a threshold equal to 80 ($MSDW_{80}$). TPR: True positive rate. FPPS: False positives per second.

in the other two cases (low TPR at +10 dB SNR, and high FPPS at 0 dB SNR); and (c) ITMS evaluated at the automatic threshold reaches an adequate compromise between high TPR and low FPPS in the three SNR conditions.

3.4. Experiment 2. Quality improvement of CAEPs

3.4.1. Methods The aim of this experiment was to evaluate the extent in which the ITMS and the MSDW methods improved the quality of cortical auditory evoked potentials (CAEPs) compared to the responses obtained without processing (RAW). The EEGs recorded in 30 normal hearing subjects (14 males, 44.73 ± 6.88 yr) were low-pass filtered (4^{th} order Butterworth, 30 Hz), and processed with the ITMS and MSDW techniques. In MSDW, since this method does not allow correction of the blink-artifact (only detection), we obtained the processed EEGs by linear interpolation of the detected blink-events boundaries. We implemented MSDW at the threshold in which best performance was observed (threshold equal to 80). The EEGs processed

with ITMS corresponded to the $y_{enhanced}(n)$ signals, described in section 2, in which the blink-artifacts were suppressed.

As presented in section 3.2, the recorded EEGs contained the neural responses evoked by 250 /da/ stimuli. In each EEG, we obtained five different CAEP signals by averaging and demeaning five blocks of 50 sweeps (EEG segments corresponding to the first 300 ms from the stimulus onset). The quality of the signals was estimated in terms of their reproducibility by calculating the correlation coefficient (r) between all possible combinations of the five CAEPs, taken two at a time (10 statistics per subject) [56]. Thus, we obtained an r-distribution of 300 statistics (30 subjects) for the RAW, MSDW, and ITMS scenarios.

Since none of the three r-distributions were normally distributed (p-values were statistically significant in the Lilliefors normality test), the three r-distributions were compared by the non-parametric Kruskal-Wallis analysis of variance test, applying the Tukey-Kramer correction for multiple comparisons. Statistic significance was achieved for p-values lower than 0.05 [57].

3.4.2. Results Figure 4.A shows an example of an unprocessed EEG segment (RAW), and processed with the MSDW and ITMS methods. This figure shows that despite both ITMS and MSDW detect all blink-events in this segment, ITMS is better at suppressing the blink-artifact. Since MSDW assumes that the shape of the artifact is triangular [51], the boundaries of the detected blink-events only include the first positive peak of the artifact. In contrast, ITMS characterizes all components of the blink-artifact waveform, and the suppression is more efficient. Figures 4.B-E show the CAEP signals obtained in each scenario in the first four subjects. The CAEP signals are presented overlapped to allow visual inspection of reproducibility. In each subject and condition, the number at the top of the charts show the mean of the correlation coefficients obtained between all possible combinations of CAEP signals taken two at a time (10 statistics). The individual results obtained in the remaining subjects are shown as supporting material in appendix C.

Figure 5 shows the raw distributions (gray-filled circles), the box plots, and the mean and standard error of the mean (errorbars) for the r-distributions in each analysed scenario. The box plots show the quartile ranges of the distributions (the notch in the boxes indicating the *median*). The *mean* values corresponding to the RAW, MSDW, and ITMS r-distributions are, respectively, 0.37, 0.54, and 0.65. The p-values shown at the top of the figure are the result of the multiple comparison test derived from the Kruskal-Wallis analysis of variance test. The results of this experiment indicate that: (a) both MSDW and ITMS methods improve the quality of CAEP signals; and (b) ITMS presents a statistically significant greater improvement (0.11 greater r-values on average) compared to MSDW.

Figure 6 shows the distributions of the inter-blink interval (IBI) and the amplitude of the blink-events detected in all subjects. This figure shows that on average (estimated as the mean between the first and the third quartile of the distribution), the subjects

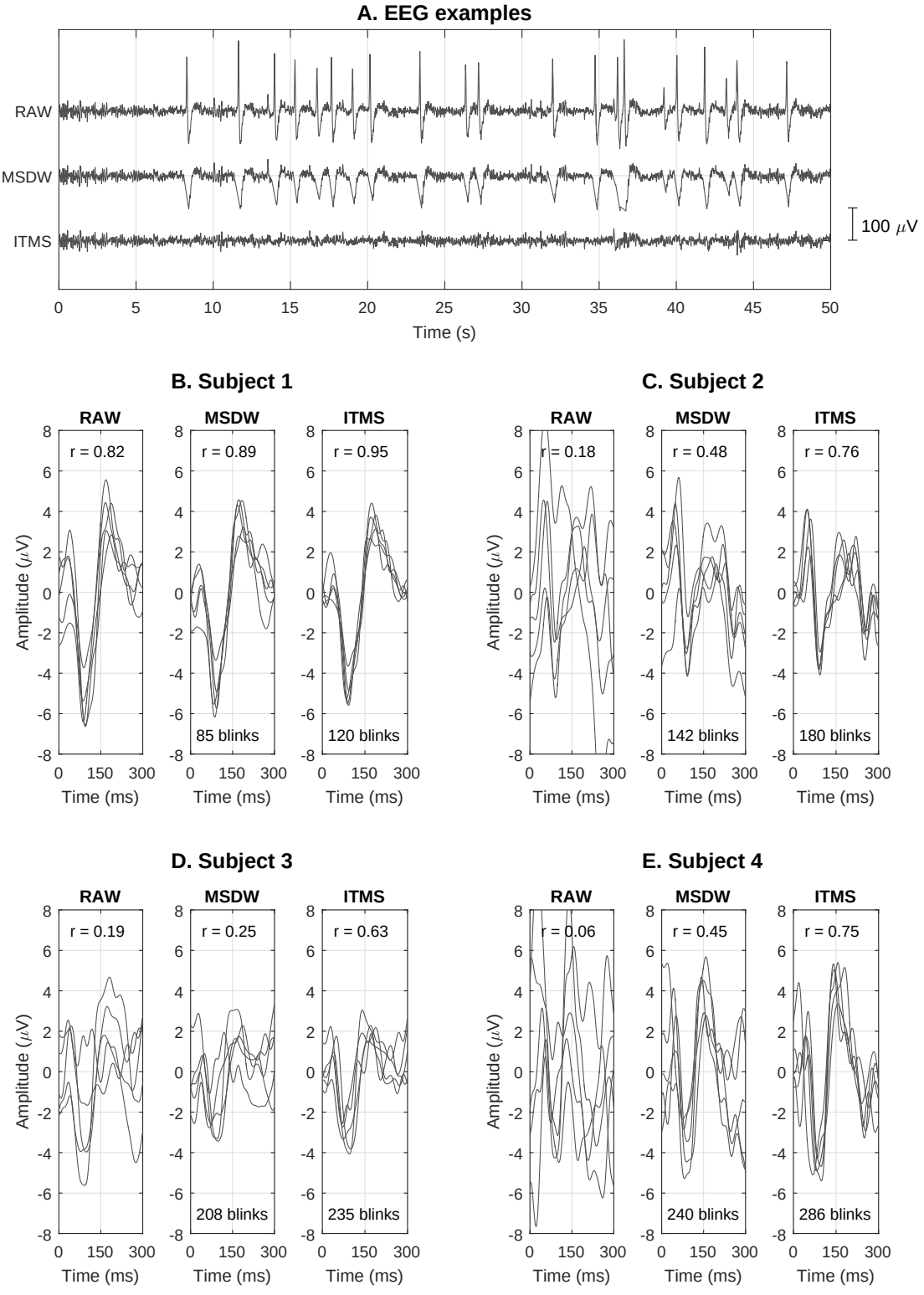

Figure 4. (A) Example of a raw EEG segment (top), and the associated EEGs processed by MSDW (middle) and ITMS (bottom). (B-E) Overlapping CAEP signals obtained in each scenario in 4 subjects. The number of detected blink-events and the mean correlation coefficient (r) between all possible combinations of the CAEP signals from each subject taken two at a time (10 statistics) are shown at the bottom and at the top of the plot respectively.

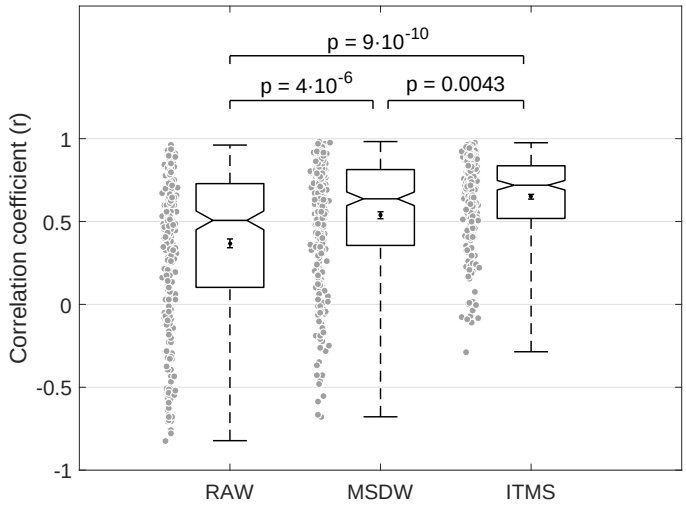

Figure 5. Raw distributions (gray-filled circles), quartile ranges (box plots), and mean and standard error of the mean (errorbars) of the r-distributions obtained for the RAW, MSDW and ITMS secenarios. Outliers of the distributions are represented with crosses. The p-values at the top of the figure show the levels of significance resulting from the multiple comparison test.

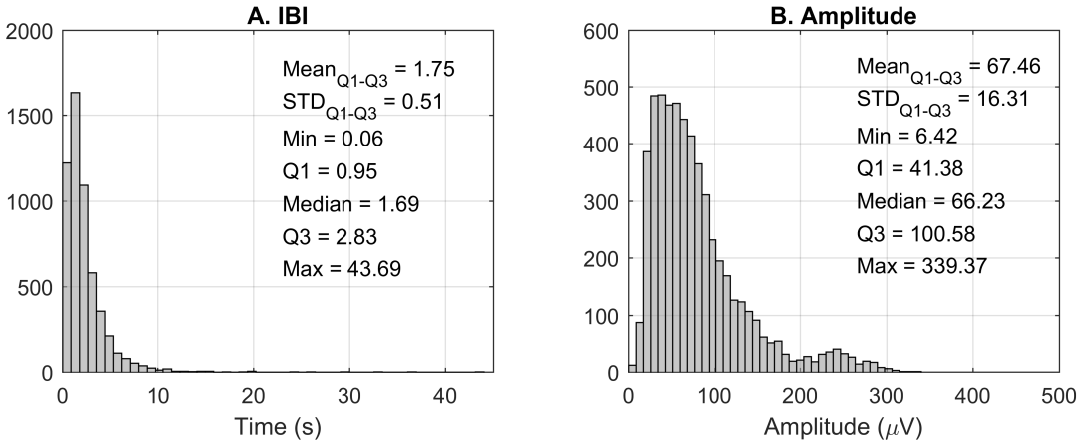

Figure 6. Histrogram of the (A) inter-blink interval (IBI) and (B) amplitude of the blink-artifacts detected in all subjects.

blinked every 1.75 seconds with an amplitude of 67.46 μV.

4. Discussion

This paper presents in detail and evaluates the performance of the Iterative Template Matching and Suppression (ITMS) technique. This paper shows that (a) ITMS presents an adequate performance in detecting and suppressing blink-artifacts from a single EEG channel; (b) it is fully automatic, since the method does not require any user setup; (c) in contrast to other methods like ICA and DWT, that decompose the EEG signals into a number of components, operate in the transformed domain, and recompose the signals,

ITMS is less invasive, since the blink-artifact correction only occurs in the contaminated EEG segments; and (d) the underlying mathematics are not complex and the method is easy to implement, as a script programmed in Matlab is provided as supplementary material.

ITMS aims to solve two classical limitations of previous methods based on template matching: the selection of the template and the estimate of the threshold. The performance of template matching is highly dependent on the template selection [51]. Previous methods used a library of blink-artifact templates of different waveforms to adapt the inter-subject variability [49, 50], however this approach presented the drawbacks of (a) generating a sufficiently large database of templates, and (b) the selected template would never perfectly match the blink-artifact waveform of the analyzed subjects. In contrast, ITMS solves the problem of template selection through an iterative process. This approach does not require a library of templates, and blink-events detection is performed using a blink-artifact template particular for each analyzed subject.

A second limitation of previously implemented template matching-based methods is that the threshold that separates the blink-events from the noise distribution was selected manually by the user [49, 50], which makes these methods inconsistent worldwide and dependent on human expertise. Moreover, this paper highlights the limitations of methods relying on manual thresholds. Firstly, the MSDW threshold suggested by the authors of this technique (threshold equal to 130) did not work well with our data, since the TPR was extremely low in all SNR scenarios (see table 1). And secondly, we observed that a threshold equal to 80 was the most appropriate in our set of real data, however, figure 3 and table 1 also show that while this threshold was appropriate in the +5 dB SNR scenario, it was not efficient when the SNR was high (low TPR) and when the SNR was low (high FPPS). In contrast, the automatic approach taken by ITMS presented an adequate blink-events detection performance irrespective of the SNR of the test.

This paper also questions the blink-artifact triangular shape assumption considered by some techniques like MSDW. The blink-artifact waveforms observed across subjects in this study presented a similar morphology, consistent with previous studies [60, 61]: an onset with an abrupt peak following a lower frequency component which extends up to 1 second approximately. Figure 4.A shows an EEG segment contaminated by a number of blink-artifacts (RAW) and the same segment corrected by the MSDW and ITMS methods. This figure shows that the triangular-shape assumption of MSDW allows detection of only the onset peak of the artifact, and therefore, the artifact cannot be completely removed. By contrast, the blink-artifact template estimated by ITMS allows an adequate characterization and suppression of the artifact, which leads to a greater improvement of the quality of the signal of interest (figure 5).

Despite MSDW only allowing blink-artifact detection, we implemented a blink-artifact correction procedure consisting of linear interpolation between the boundaries of the detected blink-artifacts. This approach was followed because, despite other

techniques having previously attempted to suppress blink-artifacts in single EEG channel applications, we did not find any alternative satisfactory option. Kanoga and Mitsukura (2014) described a method suppressing from the EEG the frequency components of the blink-events, which are estimated through a 2-step non-negative matrix factorization [60]. However, this method does not allow blink-events detection, and its performance is strongly dependent on the selection of the basis K_1 and K_2, which requires human intervention and with no procedure available to obtain an optimal selection. Rahman and Othman (2015) aimed to solve the need for an EOG reference channel in adaptive filtering by replacing this channel with a softened version of the EEG using a Savitzky-Golay filter [61]. The problem of using a low-pass version of the EEG as a reference is that relevant low frequency EEG components could be suppressed. Majmudar et al. (2015) and Khatun et al. (2016) presented a similar approach based on the discrete wavelet transform (DWT) [62, 63]. This technique basically consists of three steps: decomposing the EEG into a series of high pass and low pass filters, thresholding the coefficients, and recomposing the signal from the filtered components. The major limitation of DWT is that this technique is not efficient when the artifacts overlap in the frequency domain [21].

Four considerations must be taken into account about ITMS. First, the signal of interest and the blink-artifacts must be decorrelated, otherwise part of the signal of interest could be modeled as artifact and be suppressed from the EEG. This assumption is not valid if the test requires auditory stimuli presented at very loud levels, i.e. greater than 80 dB hearing level (HL), since these sounds may evoke an involuntary contraction of the orbicularis oculi muscle (acoustic startle reflex) [58, 59]. Second, ITMS is able to detect, characterize and suppress the artifact associated with the blink activity, but not other types of artifacts like eye saccades, muscular or cardiac activity. Nevertheless, ITMS could be implemented in conjuction with other denoising techniques. Third, the blink-artifact model $\widehat{x}_{blink}(n)$ generated by ITMS represents the LTI component of the blink-artifact signal $x_{blink}(n)$, which is unknown. ITMS introduces linear variations in the amplitude of the estimated blink-artifact template to match each blink-artifact detected in the EEG, but it does not perform other non-linear transformations on the template. The results of this study show that removing the LTI component of the blink-artifact signal improves the quality of CAEP signals significantly (figure 5). Finally, since ITMS requires the full EEG to operate, this method can only be applied in offline applications.

Although ITMS is outlined for a single EEG channel application, this method could also be scaled to a multichannel configuration. This setup would involve a first step in which blink-events detection (m_k) is carried out from a single frontal channel, as described in this paper; and a second step in which, considering the estimated m_k, the blink-artifacts are estimated and suppressed in the remaining EEG channels by applying without any iteration the processes "Template estimation", "Amplitudes estimation" and "Blink-artifact suppression" (described in section 2). The implementation of ITMS in a multichannel configuration could be approached in a future study.

Acknowledgements

The authors acknowledge Ms Ingrid Yeend (NAL: National Acoustic Laboratories, Sydney, Australia) for recruiting and carrying out the audiometry tests; and Mr Greg Stewart (NAL) for his help with the calibration of the stimuli. The authors would also like to give a special thanks to the subjects who participated in the EEG recording sessions of this study. This research was supported by grants from the National Health and Medical Research Council (grant ID 1063905), and the Hearing Industry Research Consortium.

Appendix

Supporting information associated with this article can be found in [URL].

References

[1] Sininger YS (2007). The use of Auditory Brainstem Response in screening for hearing loss and audiometric threshold prediction, in Auditory Evoked Potentials. Basic Principles and Clinical Application, Lippincott Williams & Wilkins, Baltimore, MD, 2007 (Chapter 12).

[2] Krishnaveni V, Jayaraman S, Anitha L, Ramadoss K (2006). Removal of ocular artifacts from EEG using adaptive thresholding of wavelet coefficients. *Journal of Neural Engineering* **3** 338-346.

[3] Lopes da Silva F (2013). EEG and MEG: Relevance to Neuroscience. *Neuron* **80** 1112-1128.

[4] Patel SH, Azzam PN (2005). Characterization of N200 and P300: Selected studies of the Event-Related Potential. *International Journal of Medical Sciences* **2** 147-154.

[5] Wan F, Nan W, Vai MI, Rosa A (2014). Resting alpha activity predicts learning ability in alpha neurofeedback. *Frontiers in Human Neuroscience* **8**, article 500, 7 p.

[6] Klimesch W (1996). Memory processes, brain oscillations and EEG synchronization. *International Journal of Psychophysiology* **24** 61-100.

[7] Hwang G, Jacobs J, Geller A, Danker J, Sekuler R, Kahana MJ (2005). EEG correlates of verbal and nonverbal working memory. *Behavioral and Brain Functions* **1**, 20 p.

[8] Prat CS, Yamasaki BL, Kluender RA, Stocco A (2016). Resting-state qEEG predicts rate of second language learning in adults. *Brain and Language* **157-158** 44-50.

[9] Kuhl PK (2010). Brain mechanisms in early language acquisition. *Neuron* **67** 713-727.

[10] Rothenberger A, Moll GH (1994). Standard EEG and dyslexia in children–new evidence for specific correlates? *Acta Paedopsychiatrica* **56** 209-218.

[11] Boutros NN, Lajiness-O'Neill R, Zillgitt A, Richard AE, Bowyer SM (2015). EEG changes associated with autistic spectrum disorders. *Neuropsychiatric Electrophysiology* **1:3**, 20 p.

[12] Sharma M, Purdy SC, Kelly AS (2014). The contribution of speech-evoked cortical auditory evoked potentials to the diagnosis and measurement of intervention outcomes in children with auditory processing disorder. *Seminars in Hearing* **35** 51-64.

[13] Gratton G (1998). Dealing with artifacts: the EOG contamination of the event-related brain potential. *Behavior Research Methods, Instruments, and Computers* **30** 44-53.

[14] Haggemann D, Naumann E (2001). The effects of ocular artifacts on (lateralized) broadband power in the EEG. *Clinical Neurophysiology* **112** 215-231.

[15] Urigüen JA, Garcia-Zapirain G (2015). EEG artifact removal - State-of-the-art and guidelines. *Journal of Neural Engineering* **12** 031001, 23 p.

[16] Gratton G, Coles MGH, Donchin E (1983). A new method for off-line removal of ocular artifact. *Electroencephalography and Clinical Neurophysiology* **55** 468-484.

[17] Croft RJ, Barry RJ (2000). EOG correction of blinks with saccade coefficients: a test and revision of the aligned-artefact average solution. *Clinical Neurophysiology* **111** 444-451.

[18] Wallstrom GL, Kass RE, Miller A, Cohn JF, Fox NA (2004). Automatic correction of ocular artifacts in the EEG: a comparison of regression-based and component-based methods. *International Journal of Psychophysiology* **53** 105-119.

[19] Croft RJ, Chandler JS, Barry RJ, Cooper NR, Clarke AR (2005). EOG correction: a comparison of four methods. *Psychophysiology* **42** 16-24.

[20] Pham TTH, Croft RJ, Cadusch PJ, Barry RJ (2011). A test of four EOG correction methods using an improved validation technique. *International Journal of Psychophysiology* **79** 203-210.

[21] Sweeney KT, Ward TE, McLoone SF (2012). Artifact removal in physiological signals-practices and possibilities. *IEEE Transactions on Information Technology in Biomedicine* **16** 488-500.

[22] Croft RJ, Barry RJ (2000). Removal of ocular artifacts from the EEG: A review. *Neurophysiologie Clinique/Clinical Neurophysiology* **30** 5-19.

[23] Hesse CW, James CJ (2006). On semi-blind source separation using spatial constraints with applications in EEG analysis. *IEEE Transactions on Biomedical Engineering* **53** 2525-2534.

[24] Mennes M, Wouters H, Vanrumste B, Lagae L, Stiers P (2010). Validation of ICA as a tool to remove eye movement artifacts from EEG/ERP. *Psychophysiology* **47** 1142-1150.

[25] Zhou W, Gotman J (2009). Automatic removal of eye movement artifacts from the EEG using ICA and the dipole model. *Progress in Natural Science* **19** 1165-1170.

[26] Davies ME, James CJ (2007). Source separation using single channel ICA. *Signal Processing* **87** 1819-1832.

[27] Romero S, Mañanas MA, Barbanoj MJ (2008). A comparative study of automatic techniques for ocular artifact reduction in spontaneous EEG signals based on clinical target variables: A simulation case. *Computers in Biology and Medicine* **38** 348-360.

[28] Kierkels JJM, van Boxtel GJM, Vogten LLM (2006). A model-based objective evaluation of eye movement correction in EEG recordings. *IEEE Transactions on Biomedical Engineering* **53** 246-253.

[29] Joyce CA, Gorodnitsky IF, Kutas M (2004). Automatic removal of eye movement and blink artifacts from EEG data using blind component separation. *Psychophysiology* **41** 313-325.

[30] Delorme A, Makeig S (2004). EEGLAB: an open source toolbox for analysis of single-trial EEG dynamics. *Journal of Neuroscience Methods* **134** 9-21.

[31] Jung TP, Humphries C, Lee TW, Makeig S, Mckeown M, Iragui V, Sejnowski TJ (1998). Removing electroencephalographic artifacts: Comparison between ICA and PCA. *Neural Networks for Signal Processing VIII, Proceedings of the 1998 IEEE Signal Processing Society Workshop*, 63-72.

[32] Anderer P, Roberts S, Schlögl A, Gruber G, Klösch G, Hermann W, Rappelsberger P, Filz O, Barbanoj M, Dorffner G, Saletu B (1999). Artifact processing in computerized analysis of sleep EEG - A review. *Neuropsychobiology* **40** 150-157.

[33] Hoffmann S, Falkenstein M (2008). The correction of eye blink artefacts in the EEG: A comparison of two prominent methods. *PLoS ONE* **3**:e3004, 11 p.

[34] Van Dun B, Dillon H, Seeto M (2015). Estimating hearing thresholds in hearing-impaired adults through objective detection of cortical auditory evoked potentials. *Journal of the American Academy of Audiology* **26** 370-383.

[35] Duvinage M, Castermans T, Petieau M, Hoellinger T, Cheron G, Dutoit T (2013). Performance of the Emotiv Epoc headset for P300-based applications. *BioMedical Engineering Online* **12**:56, 15 p.

[36] Kawala-Janik A, Baranowski J, Podpora M, Piatek P, Pelc M (2014). Use of a cost-effective neuroheadset EMOTIV Epoc for pattern recognition purposes. *International Journal of Computing* **13** 25-33.

[37] Campbell AT, Choudhury T, Shaohan H, Hong L, Mukerjee MT, Rabbi M, Rajeev DSR (2010). NeuroPhone: Brain-mobile phone interface using a wireless EEG headset. *MobiHeld '10*

Proceedings of the second ACM SIGCOMM workshop on Networking, systems, and applications on mobile handhelds pp. 3-8, New Delhi, India, August 2010.

[38] Nolan H, Whelan R, Reilly RB (2010). FASTER: fully automated statistical thresholding for EEG artifact rejection. *Journal of Neuroscience Methods* **192** 152-162.

[39] Zammouri A, Aitmoussa A, Chevallier S, Monacelli E (2015). Intelligent ocular artifacts removal in a non-invasive single channel EEG recording. *Intelligent Systems and Computer Vision (ISCV)*, 7106164, 5 p, At Fez, Morocco, March 2015.

[40] Aarabi A, Kazemi K, Grebe R, Moghaddam HA, Wallois F (2009). Detection of EEG transients in neonates and older children using a system based on dynamic time-warping template matching and spatial dipole clustering. *NeuroImage* **48** 50-62.

[41] Benedetto S, Pedrotti M, Minin L, Baccino T, Re A, Montanari R (2011). Driver workload and eye blink duration. *Transportation Research Part F: Traffic Psychology and Behaviour* **14**, 199-208.

[42] Klein A, Skrandies W (2013). A reliable statistical method to detect eyeblink artefacts from electroencephalogram data only. *Brain Topography* **26** 558-568.

[43] Peng X, Xu J (2016). Hash-based line-by-line template matching for lossless screen image coding. *IEEE Transactions on Image Processing* **25**, 5601-5609.

[44] Ahuja K, Tuli P (2013). Object recognition by template matching using correlations and phase angle method. *International Journal of Advanced Research in Computer and Communication Engineering* **2** 1368-1373.

[45] Faundez-Zanuy M (2007). On-line signature recognition based on VQ-DTW. *Pattern Recognition* **40** 981-992

[46] Fu TC, Chung FL, Luk R, Ng CM (2007). Stock time series pattern matching template-based vs. rule-based approaches. *Engineering Applications of Artificial Intelligence* **20** 347-364.

[47] Gong, X, Si YW (2013). Comparison of subsequence pattern matching methods for financial time series. *9th International Conference on Computational Intelligence and Security (CIS), Dec 2013*, 6746375, 154-158.

[48] Skoumal RJ, Brudzinski MR, Currie BS (2015). Distinguishing induced seismicity from natural seismicity in Ohio: Demonstrating the utility of waveform template matching. *Journal of Geophysical Research B: Solid Earth* **120** 6284-6296.

[49] Bizopoulos PA, Al-Ani T, Tsalikakis DG, Tzallas AT, Koutsouris DD, Fotiadis DI (2013). An automatic electroencephalography blinking artifact detection and removal method based on template matching and ensemble empirical mode decomposition. *35th Annual International Conference of the IEEE EMBS, Osaka, Japan, 3-7 July 2013*, 6610883, pp. 5853-5856.

[50] Chang WD, Im CH (2014). Enhanced template matching using dynamic positional warping for identification of specific patterns in electroencephalogram. *Journal of Applied Mathematics*, Article ID 528071, 7 p.

[51] Chang WD, Cha HS, Kim K, Im CH (2016). Detection of eye blink artifacts from single prefrontal channel electroencephalogram. *Computer Methods and Programs in Biomedicine* **124** 19-30.

[52] Turin GL (1960). An introduction to matched filters. *IRE Transactions on Information Theory* **6** 311-329.

[53] Kim S, McNames J (2007). Automatic spike detection based on adaptive template matching for extracellular neural recordings. *Journal of Neuroscience Methods* **165** 165-174.

[54] Huber PJ (2005). Robust statistics, in Wiley Series in Probability and Statistics, New York: John Wiley & Sons, Inc.

[55] Boersma P, Weenink D (2016). Praat: doing phonetics by computer [Computer program]. Version 6.0.17, retrieved 27 April 2016 from www.praat.org.

[56] Elberling C, Don M (2007). Detecting and assessing synchronous neural activity in the temporal domain (SNR, response detection), in Auditory Evoked Potentials. Basic Principles and Clinical Application, Lippincott Williams & Wilkins, Baltimore, MD, (Chapter 5).

[57] Ludbrook J (2008). Statistics in biomedical laboratory and clinical science: Applications, issues and pitfalls. *Medical Principles and Practice* **17** 1-13.

[58] Hahlbrock KH (1962). Auropalpebral-reflex audiometry. *International Journal of Audiology* **1** 261-264.

[59] Ramirez-Moreno DF, Sejnowski, TJ (2012). A computational model for the modulation of the prepulse inhibition of the acoustic startle reflex. *Biological Cybernetics* **106** 169-176.

[60] Kanoga S, Mitsukura Y (2014). Eye-blink artifact reduction using 2-step nonnegative matrix factorization for single-channel electroencephalografic signals. *Journal of Signal Processing* **18** 251-257.

[61] Rahman FA, Othman MF (2015). Eye blinks removal in single-channel EEG using Savitzky-Golay referenced adaptive filtering: a comparison with independent component analysis method. *ARPN Journal of Engineering and Applied Sciences* **10** 18147-18154.

[62] Majmudar CA, Mahajan R, Morshed BI (2015). Real-time hybrid ocular artifact detection and removal for single channel EEG. *IEEE International Conference on Electro/Information Technology (EIT), 21-23 May 2015*, pp. 330-334.

[63] Khatun S, Mahajan R, Morshed BI (2016). Comparative study of wavelet-based unsupervised ocular artifact removal techniques for single-channel EEG data. *IEEE Journal of Translational Engineering in Health and Medicine* **4** 1-8.